AD_____

Award Number:  DAMD17-03-1-0119


TITLE:  Ultrasound Activated Contrast Imaging For Prostate Cancer Detection


PRINCIPAL INVESTIGATOR:  Flemming Forsberg, Ph.D.


CONTRACTING ORGANIZATION:  Thomas Jefferson University
                          Philadelphia, PA  19107


REPORT DATE:  March 2006


TYPE OF REPORT:  Annual


PREPARED FOR:  U.S. Army Medical Research and Materiel Command
               Fort Detrick, Maryland  21702-5012

# REPORT DOCUMENTATION PAGE

Public reporting burden for this collection of information is estimated to average 1 hour per response, including the time for reviewing instructions, searching existing data sources, gathering and maintaining the data needed, and completing and reviewing this collection of information. Send comments regarding this burden estimate or any other aspect of this collection of information, including suggestions for reducing this burden to Department of Defense, Washington Headquarters Services, Directorate for Information Operations and Reports (0704-0188), 1215 Jefferson Davis Highway, Suite 1204, Arlington, VA 22202-4302. Respondents should be aware that notwithstanding any other provision of law, no person shall be subject to any penalty for failing to comply with a collection of information if it does not display a currently valid OMB control number. **PLEASE DO NOT RETURN YOUR FORM TO THE ABOVE ADDRESS.**

| 1. REPORT DATE *(DD-MM-YYYY)* 01-03-2006 | 2. REPORT TYPE Annual | 3. DATES COVERED *(From - To)* 1 MAR 2005 - 28 FEB 2006 |
|---|---|---|

| 4. TITLE AND SUBTITLE | 5a. CONTRACT NUMBER |
|---|---|
| Ultrasound Activated Contrast Imaging For Prostate Cancer Detection | |
| | 5b. GRANT NUMBER DAMD17-03-1-0119 |
| | 5c. PROGRAM ELEMENT NUMBER |
| 6. AUTHOR(S) Flemming Forsberg, Ph.D. | 5d. PROJECT NUMBER |
| | 5e. TASK NUMBER |
| E-mail: flemming.forsberg@jefferson.edu | 5f. WORK UNIT NUMBER |

| 7. PERFORMING ORGANIZATION NAME(S) AND ADDRESS(ES) Thomas Jefferson University Philadelphia, PA 19107 | 8. PERFORMING ORGANIZATION REPORT NUMBER |
|---|---|

| 9. SPONSORING / MONITORING AGENCY NAME(S) AND ADDRESS(ES) U.S. Army Medical Research and Materiel Command Fort Detrick, Maryland 21702-5012 | 10. SPONSOR/MONITOR'S ACRONYM(S) |
|---|---|
| | 11. SPONSOR/MONITOR'S REPORT NUMBER(S) |

**12. DISTRIBUTION / AVAILABILITY STATEMENT**
Approved for Public Release; Distribution Unlimited

**13. SUPPLEMENTARY NOTES**
Original contains color plates: All DTIC reproductions will be in black and white.

**14. ABSTRACT**

The current project proposes to develop a novel ultrasound contrast imaging technique (called EEI) for better visualization of the microvessels, which are characteristic of the neovasculature associated with prostate cancer.
The new zero-thickness interface model was used to simulate the dual pulse imaging mode associated with EEI. While results at an imaging frequency of 7.5 MHz were somewhat in agreement with measurements, the enhancement was unrealistically high (20-35 dB). Further work is ongoing to improve upon the model by incorporating the growth and dissolution of microbubbles. Initial simulation results indicate that the shell elasticity plays a vital role in the growth as well as dissolution of the bubbles.
The pulse-echo system was used to perform further *in vitro* EEI measurements at 7.5 MHz and initial experiments were conducted with 3 contrast agents. The contrast agent Definity produce no enhancement in EEI mode at any of the concentrations studied, while around 6 dB of enhancement was measured with another contrast agent Therimage at the second harmonic frequency at a 20 µl/l concentration.

**15. SUBJECT TERMS**
Prostate Cancer, Ultrasound Imaging, Ultrasound Contrast Agent

| 16. SECURITY CLASSIFICATION OF: | | | 17. LIMITATION OF ABSTRACT | 18. NUMBER OF PAGES | 19a. NAME OF RESPONSIBLE PERSON USAMRMC |
|---|---|---|---|---|---|
| a. REPORT U | b. ABSTRACT U | c. THIS PAGE U | UU | 15 | 19b. TELEPHONE NUMBER *(include area code)* |

# 3. TABLE OF CONTENTS

# 4.  INTRODUCTION

The diagnosis of prostate cancer is currently based on an elevated prostate-specific antigen (PSA) level or abnormal digital rectal examination findings confirmed by needle biopsy of the prostate.  It is estimated that the number of men subjected to biopsy of the prostate in the U.S. in 2001 exceeded 600,000 [1].  Unfortunately, the frequency of positive biopsy findings, for most screening populations, was as low as one in three to one in four.  Therefore, an accurate, noninvasive diagnostic imaging examination of the prostate is needed to reduce the number of biopsies or even to replace biopsy.

A sextant biopsy of the prostate, consisting of the acquisition of six biopsy cores, can miss clinically detectable prostate caner in up to 34% of men.  Among patients with an elevated PSA level and a negative initial sextant biopsy finding, repeat biopsy demonstrates the presence of malignancy in approximately 20%-30% [2].  However, each additional biopsy is associated with a small incremental risk of hemorrhage and infection.  Thus, an accurate, noninvasive imaging technique is useful for targeted biopsy guidance in order to reduce the number of biopsies in each prostate.

The sensitivity and specificity of ultrasound imaging can be improved by intravenous injection of vascular contrast agents consisting of encapsulated gas microbubbles [3].   Due to encapsulation, these agents are stable enough to pass through the pulmonary circulation and flow in intravascular space for at least several minutes.  However, encapsulation imposes severe restrictions on the oscillations of contrast bubbles.  Based on de Jong's numerical model [4], our calculations indicate that the incident acoustic pressure amplitude for an albumin-encapsulated Abunex® bubble is 18 times greater than that for a free bubble if the two bubbles oscillate with the same relative amplitude at their resonant frequency of 2 MHz.  Hence, scattering can be greatly enhanced if encapsulated bubbles become free bubbles.  According to the Rayleigh's approximation, the fundamental scattering cross-section of an air bubble is more than 200 times (47 dB) greater than that for an Abunex bubble of the same size.  Furthermore, the enhancement in second or sub- harmonic scattering cross-section must be even much greater because encapsulation dampens nonlinear oscillations to a much greater degree.

Unlike current ultrasound imaging modalities employing only an imaging field, the proposed technique utilizes two acoustic fields: the activation field for intermittently activating contrast bubbles and the imaging field, applied shortly afterwards, for acquiring harmonic or subharmonic images with significantly enhanced scattering signals from activated contrast bubbles.  This new imaging mode is referred to as Excitation Enhanced Imaging (EEI) [5].  Based on previous work on ultrasound-induced contrast scattering enhancement and contrast-assisted ultrasonographic detection of human and canine prostate cancer, the hypotheses of this study are: (1) contrast microbubbles can be ultrasonically activated to achieve marked backscattering enhancement, and (2) the detection of prostate cancer can be improved using the proposed ultrasonographic technique.  It is well known that a free bubble resonating at the insonation frequency is the optimal acoustic scatterer.  Hence, the activation field will consist of a release pulse for effectively releasing free bubbles from encapsulated contrast bubbles and an excitation pulse for shifting the free bubbles to the resonance size corresponding to a pre-selected imaging frequency.

# 5.  BODY

It is the central hypothesis of this study that contrast microbubbles can be activated and backscattering enhanced markedly.  The activation field will produce the optimal acoustic scatterers, i.e., free bubbles resonant around a pre-selected imaging frequency.  In the proposed study, both the modeling and measurement will help us to determine optimal contrast agents and develop optimal activation pulse sequences enhancing backscattered second and sub-harmonic signals by a factor of 2 to 16, i.e., by 6 to 24 dB.  The other hypothesis of this study is that prostate cancer can be detected using the proposed ultrasonographic technique.  This hypothesis will be tested using an established canine prostate tumor model.  The specific tasks of the project (as presented in the original Statement of Work) can be found in Appendix I.

First an outline of the methods applied will be given followed by a presentation of the results to date.  Finally, the conclusions and future directions of the research will be discussed.

## 5.1  Methods

*Contrast microbubble modeling*
We have adopted a Newtonian rheology, i.e., only viscous interfacial stresses are considered (see [6] for details) to develop a new simulation model of contrast bubbles based on a modified Rayleigh-Plesset type equation (as detailed in the previous report and in [7]).  However, when this model was expanded to account for EEI effects, the model did not predict excperiemntal results well (see previous report).  Hence, we have attempted to produce a more realistically model incorporating bubble growth and dissolution via rectified diffusion, and these efforts have been submitted for publication [8].

Here we model the bubble shell as a semi-permeable membrane, with two gases air and octafluoropentane (OFP) inside the bubble.  The dissolution time scale and the growth of the bubbles have been studied for varying mole fraction of the osmotic agent (OFP), surface tension, shell permeability, and air saturation level in the bulk. Also, elastic shell has been considered and it has been found that shell elasticity plays a vital role in the dissolution and growth of these bubbles.  The dissolution process as said earlier is delayed due to the presence of the shell.  Here we assume the process of dissolution to be very slow and hence dissolution by steady diffusion is being considered.

Let the concentration of the gas in the liquid be C.  Using the steady state diffusion equation and appropriate boundary conditions allows us to arrive at the following expression:

$$\frac{d(R^3 C_g)}{dt} = 3R^2 k_g \frac{(C_\infty - C_w)}{\left(\dfrac{k_g}{\alpha} + R\right)} \tag{1}$$

where $k_m$ and $k_g$ are the coefficients of diffusivity of the gas through membrane and the liquid, respectively, while $\delta$ is the thickness of the membrane (shell) and $\alpha$ is the ratio of the $k_m/\delta$. The instantaneous radius of the bubble is denoted $R$, while $C_w$ & $C_R$ are the concentration of the gas on the inner and the outer wall of the bubble, respectively.

If we consider 2 different gases fluorocarbon and air in the bubble, then equation (1) can be written as equation (2) and (3) for fluorocarbon (index $F$) and air (index $A$), respectively.

$$\frac{d(R^3 C_F)}{dt} = 3R^2 k_F \frac{(C_{F(\infty)} - C_{F(w)})}{\left(\dfrac{k_F}{\alpha_F} + R\right)} \tag{2}$$

$$\frac{d(R^3 C_A)}{dt} = 3R^2 k_A \frac{(C_{A(\infty)} - C_{A(w)})}{\left(\dfrac{k_A}{\alpha_A} + R\right)} \tag{3}$$

After some mathematical manipulations these equations can be reduced to [8]:

$$\frac{dF}{d\tau} = \frac{-3 L_F F}{\rho\left(\dfrac{k_F}{\alpha_F R_o} + \rho\right)} \tag{4}$$

$$\frac{dA}{d\tau} = \frac{-3 \xi L_A (A - \rho^3)}{\rho\left(\dfrac{k_A}{\alpha_A R_o} + \rho\right)} \tag{5}$$

$$F + A = \rho^2 (\mu + \rho) \tag{6}$$

where $L$ represents the Ostwald coefficient, $R_o$ is the initial bubble radius and the remaining variables are expressed as dimensionless parameters involving surface tension and the partial gas pressures [8]. The initial conditions are:

$$\rho(0) = 1 \tag{7}$$

$$A(0) + F(0) = 1 + \mu \tag{8}$$

$$\frac{F(0)}{A(0) + F(0)} = X_F \tag{9}$$

These efforts represent the continuation of task 1c and the start of task 1e (see original SOW in the Appendix).

*Elasticity effects*

If we consider the shell to be elastic with shell elasticity $E^S$ and the equilibrium radius to be the initial radius $R_o$, doing pressure balance [9] we have

$$(C_A + C_F)R_G T = P_A + P_F = \frac{2\sigma}{R} + P_{atm} + \frac{2E^S}{R}\left[\left(\frac{R}{R_o}\right)^2 - 1\right] \tag{10}$$

By defining:

$$\gamma = \frac{2E^S}{P_{atm}R_o} \tag{11}$$

equation (10) can be re-written in the following form:

$$F + A = \mu\rho^2 + \rho^3 + \gamma(\rho^4 - \rho^2) \tag{12}$$

Notice that if surface tension is set to zero in equation (10) the minimum value for the ratio $R/R_0$ is 1. When $R/R_0$ equals 1, the elasticity term vanishes in the equation (10) and the inside pressure becomes equal to the atmospheric pressure.

*In Vitro experiments*

A system was built to perform EEI and measure the enhancement of scattered signals from contrast microbubbles in a water bath with three single-element spherically-focused transducers (Staveley, East Hartford, CT, USA), as shown in Figure 1 (and described in the previous report). An excitation transducer (1.1 MHz) with a diameter of 2.5 cm and a focal length of 5.0 cm was used for conditioning microbubbles and a pair of small broadband imaging transducers (with center frequencies of 7.5 MHz), for detecting these microbubbles before and after conditioning. The excitation transducer was driven by a programmable arbitrary function generator (LW420; LeCroy, Chestnut Ridge, NY, USA) through a 500 W power amplifier (A-500; ENI, Rochester, NY, USA). Unfortunately, this power amplifier broke beyond repair halfway through the year. After 4 months of attempting repairs, we managed to secure funds from other sources to purchase a replacement unit. Getting the purchase order approved took an additional 2 months, before a 3100L power amplifier (ENI, Rochester, NY, USA) was acquired instead. This amplifier covers the frequency range of 125 kHz to 125 MHz providing 50 dB gain for up to 100 W input. Nonetheless the project was delayed somewhat by this equipment problem.

The remainder of the setup was, as previously described, based on one imaging transducer was used to transmit imaging pulses produced by a programmable function generator (8116A; Hewlett Packard, Santa Clara, CA, USA) and a broadband power amplifier (325LA; ENI) and another was employed to receive signals scattered from the contrast microbubbles. The scattered signals were amplified and then acquired using a digital oscilloscope (9350AM; LeCroy, Chestnut Ridge, NY, USA). A time modulus (AV-1023-C; Avtech Electosystems, Ogdensberg, NY, USA) was used to synchronize the delay between the conditioning and imaging pulses. The command delivery to the function generators and the data transfer from the digital oscilloscope were controlled by LabView® (National Instruments, Austin, TX, USA).
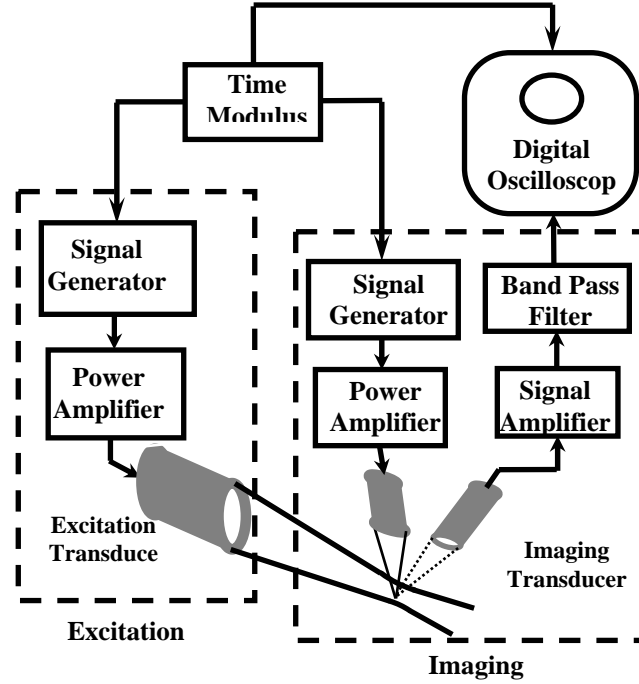
***Figure 1.*** *Experimental set-up for EEI enhancement measurement. An excitation transducer was used to condition contrast microbubbles and a pair of broadband transducers (one for transmission and another for reception, perpendicular to each other and to the excitation transducer) were employed to detect the conditioned microbubbles.*

Three different types of contrast agents were tested: a) Sonazoid® (GE Healthcare, Oslo, Norway), a lipid-coated contrast agent containing a PFC gas (this agent was studied to establish a baseline performance); b) Definity® (Bristol-Myers Squibb Diagnostic Imaging, N Bilerica, MA, USA), a lipid-shelled agent filled with octafluoropropane; and c) Therimage (Focus Therapeutics LLC, Media, PA, USA), an experimental, surfactant stabilized agent consisting of air-filled microbubbles. During the experiments, contrast agents were diluted in water and a magnetic stirrer was used to maintain mixture. Concentrations of 1, 10, 20 and 30 μl of contrast agent per liter of water were tested. An excitation amplitude of 1.2 MPa was used along with an excitation pulse length of 16 cycles operating at pulse repetition frequency (PRF) of 2 Hz. The delay between the excitation and detection pulses was 100 μs.

*In vitro* experiments were conducted at ambient temperature (22° C). For each enhancement measurement, spectra of scattered imaging signals from unconditioned and conditioned contrast microbubbles were acquired. The average spectrum for regular contrast microbubbles (before conditioning) was obtained at a given PRF based on a sequence of 64 scattered signals from transmit imaging pulses. The same imaging pulse was transmitted with a given delay after each condition pulse for 64 times (at the same PRF), so that the averaged spectrum for the conditioned microbubbles was obtained. This represents the continuation of tasks 1d and 1e (see original SOW in the Appendix).

As mentioned in last year's report, an initial version of the EEI software was implemented on two ultrasound scanners. One platform was the state-of-the-art, all digital, flagship ultrasound scanner from GE: the Logiq 9 (GE Healthcare, Milwaukee, WI). The second platform selected was an AN2300 digital ultrasound engine (Analogic Corporation, Peabody, MA). This represents the initiation of tasks 2c and 2d as outlined in the original SOW (see the Appendix) and has now been published in a peer-reviewed journal [9].

5.2  Results and Discussion

The new model of bubble growth and dissolution was implemented in Matlab (The Mathworks, Natick, MA). The variation of the $R/R_o$ with time for varying $X_F$ (where $X_F = 1$ indicates no air and $X_F = 0$ indicates no fluorocarbon inside the bubble) is shown in the Figure 2. The outside medium is saturated with air void of the perfluorocarbon. As the mole fraction of the osmotic agent (fluorocarbon) goes on increasing the growth gets bigger and the dissolution time keeps on increasing [10]. This causes initial bubble growth due to the sudden ingression of the air into the bubble [11], since the coefficient of diffusivity of the air is higher than that of perfluorocarbon.

Figure 3 shows the change in $R/R_o$ as a function of time for bubbles with no shell, a permeable and a less permeable shell ($X_F = 1$). As the permeability of the shell decreases the life time of the bubble increases from around 10 seconds for the free bubble to couple of minutes for a bubble with a less permeable shell. The free bubble (i.e., without a shell) can be considered a case of a shell with infinite permeability. The thickness of the shell can be increased to reduce the permeability (inversely proportional to shell thickness) and, hence, increase the life time of a bubble.
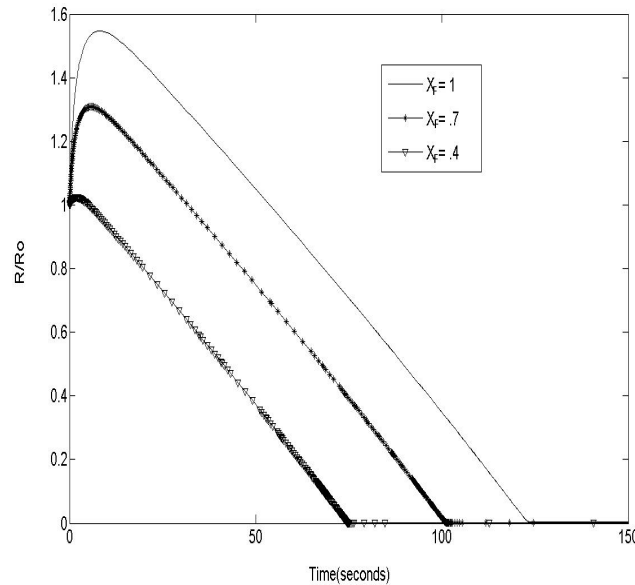


*Figure 2.* *The variation in $R/R_o$ with time for varying mole fractions of perfluorocarbon assuming a permeable shell and $f = 1$.*
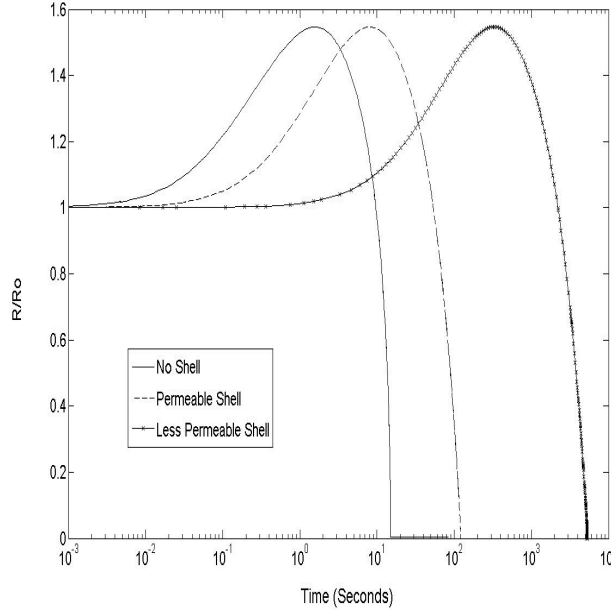
9

*Figure 3.* *Changes in R/R₀ over time for different shell types.*

The effect of the elasticity term introduced in equation (10) is demonstrated in Figure 4. When the elasticity is reduced by a factor 100 the bubble grows by 2.2 times even though there is no extra pressure inside the bubble to drive the gases out of the bubble. Notice that $R/R_o$ does not achieve values below 1 as there is no $\sigma$ to make inside pressure higher.
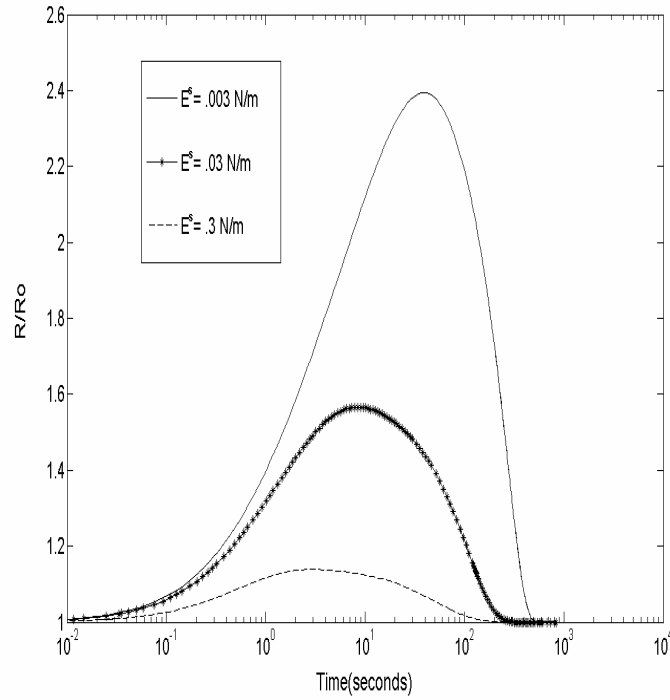


*Figure 4.* *R/R₀ plotted over time for varying $E^S$ values (using a permeable shell and $\sigma = 0$ N/m).*

In contrast Figure 5 shows $R/R_0$ for the same elasticity parameter and an $\sigma$ of *0.7* N/m, which allows the inside pressure to be still higher than the outside pressure for $R/R_0$ of 1. However, if $R/R_0$ is less than 1 in equation (10) the elasticity term becomes negative and acts towards decreasing the pressure inside the bubble. Nonetheless the surface tension term will drive the gas out of the bubble provided it dominates the elasticity parameter. If the elasticity term dominates the surface tension term then the bubble will not dissolve as can be seen for the case $E^s = .3$ N/m in Figure 5. Hence, the elasticity term competes with the surface tension term and plays a vital role in the growth as well as dissolution of the bubble, which is an important new observation that our model has provided.

The ability of our simulation model to simulate the dynamic behavior of Sonazoid microbubbles during EEI was also examined as shown in Figure 6. At an imaging frequency of 7.5 MHz the model reproduced the experimental results to some degree showing 20 and 35 dB enhancement at the fundamental and the harmonic frequencies, respectively, due to the excitation field. However, this is much higher values of enhancement than measured experimentally and enhancement is also seen at other frequencies than at 7.5 and 15 MHz. Currently, efforts are ongoing to produce a more realistic model.

The change in scattered signal strength before and after the excitation pulse (i.e., the enhancement obtained with EEI relative to standard contrast imaging) was measured for different concentrations using the pulse-echo system outlined in Figure 1. No enhancement was found for the contrast agent Definity. However, for the contrast agent Therimage we measured 4.6 dB enhancement at the fundamental frequency and 5.6 dB at the harmonic frequency as demonstrated in Figure 7 obtained at 7.5 MHz (i.e. a realistic imaging frequency for the prostate) following conditioning with 1.2 MPa excitation pulses (1.1 MHz and 16 cycles) at 2 Hz PRF. Imaging pulses (36 cycles, 7.5 MHz and 0.1 MPa) were transmitted, with a delay of 100 μs between the conditioning pulse and the detection pulse. .
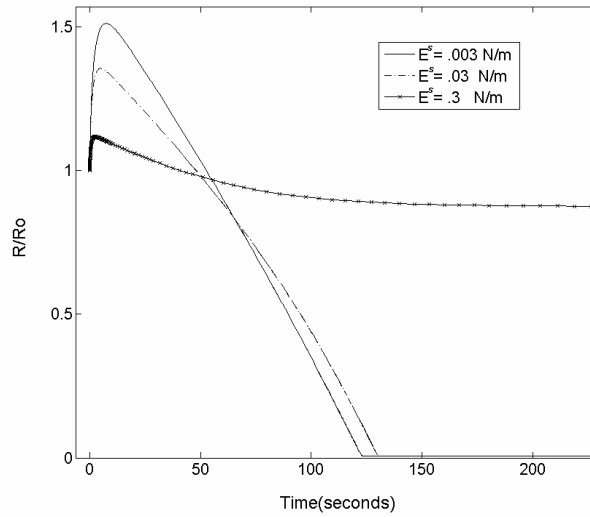


**Figure 5**. *$R/R_0$ plotted over time for varying $E^S$ values (using a permeable shell, $\sigma = 0.7$ N/m and $f = 1$).*
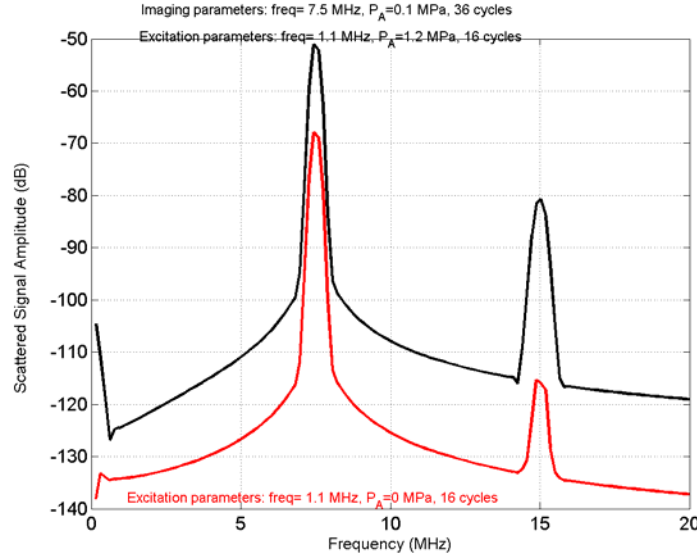
*Figure 6.* *Simulation of enhancement from Sonazoid in EEI mode using 1.1 MHz excitation at 1.2 MPa, imaging at 7.5 MHz. More than 20 dB enhancement occurs at the fundamental and the harmonic frequency.*
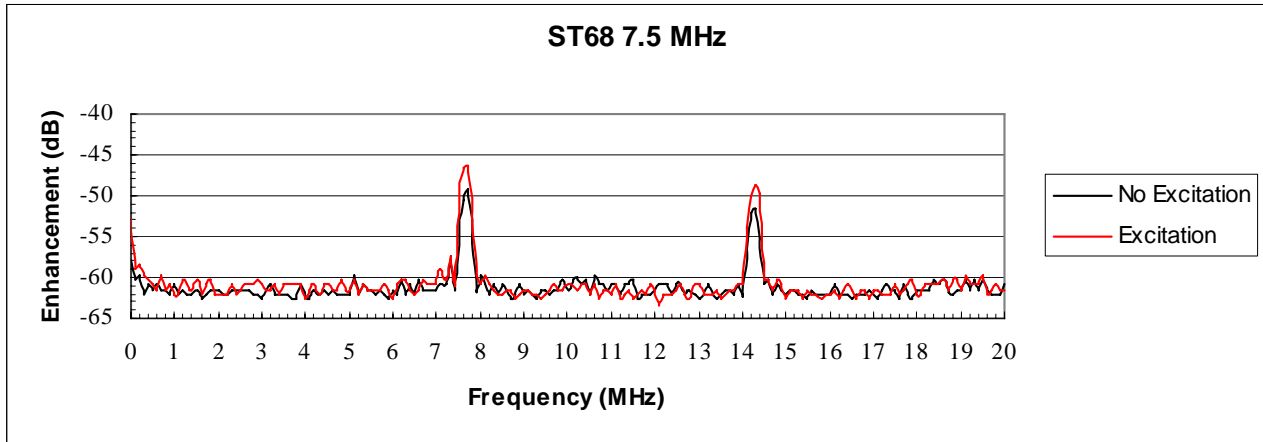


*Figure 7.* *Measurement of enhancement from Therimage (formerly known as ST68) in EEI mode using 1.1 MHz excitation at 1.2 MPa, imaging at 7.5 MHz, 2 Hz PRF obtained at 22°C. Notice, that marked enhancement ~6 dB occurs at the harmonic frequency.*

## 6.    KEY RESEARCH ACCOMPLISHMENTS

- The new zero-thickness interface model was expanded to describe the dual pulse mode of EEI, but further work is necessary.
- The growth and dissolution of microbubbles was simulated.
- The shell elasticity plays a vital role in the growth as well as dissolution of the bubbles.
- A dual-transducer pulse-echo system was used to perform EEI.

- Initial experiments were conducted at 7.5 MHz with 3 contrast agents.
- Concentration dependencies were studied.
- Up to 5.6 dB of enhancement at the second harmonic was measured at 22° C for Therimage when imaged at 7.5 MHz.
- There was slightly less enhancement (4.6 dB) occurring at the fundamental frequency.

# 7.    REPORTABLE OUTCOMES

K. Sarkar, W. T. Shi, D. Chatterjee, F. Forsberg.  Characterization of ultrasound contrast microbubbles using in vitro experiments and viscous and viscoelastic interface models for encapsulation.  *J Acoust Soc Am,* vol. 118, vol 118, no. 1, pp. 539-550, 2005.

F. Forsberg, W. T. Shi, M. M. Knauer, A. L. Hall, C. Vecchio, R. Bernardi.  Real time excitation enhanced ultrasound contrast imaging.  *Ultrasonic Imaging*, vol. 27, no. 2, pp. 65-74, 2005.

K. Sarkar, P. Jain.  Growth and dissolution of a shelled bubble applicable in the medical field.  Submitted to *J Acoust Soc Am*, May, 2006.

# 8.  CONCLUSIONS

The new zero-thickness interface model was used to simulate the dual pulse imaging mode associated with EEI.  While results at an imaging frequency of 7.5 MHz were somewhat in agreement with measurements, the enhancement was unrealistically high (20-35 dB).  Further work is ongoing to improve upon the model by incorporating the growth and dissolution of microbubbles.  Initial simulation results indicate that the shell elasticity plays a vital role in the growth as well as dissolution of the bubbles.

The pulse-echo system was used to perform further *in vitro* EEI measurements at 7.5 MHz and initial experiments were conducted with 3 contrast agents.  Definity produce no enhancement in EEI mode at any of the concentrations studied, while around 6 dB of enhancement was measured with Therimage at the second harmonic frequency at a 20 μl/l concentration.

In summary, task 1 has been almost completed while task 2 is ongoing, but due to the delay caused by the equipment problems the project is approximately 10 months behind schedule.  Consequently, a one year no cost extension was requested and has been granted to allow us to complete this project.

# 9.  REFERENCES

1.   Halpern EJ, Frauscher F, Forsberg F, Nazarian LN, O'Kane P, Gomella LG. High-frequency Doppler US of the prostate: effect of patient position. *Radiology,* 222:634-639, 2002.

2.   Pryor MB, Schellhammer PF.  The pursuit of prostate cancer in patients with a rising prostate-specific antigen and multiple negative transrectal ultrasound-guided prostate biopsies. *Clin Prostate Cancer*, 1:172-176, 2002.

3.   Goldberg BB, Raichlen JS, Forsberg F. *Ultrasound Contrast Agents: Basic Principles and Clinical Applications* (2nd Ed). Martin Dunitz Ltd., England, 2001.

4.   de Jong N, Cornet R, Lancee CT.  Higher harmonics of vibrating gas-filled microspheres. part one: simulations. *Ultrasonics*, 32:447-453, 1994.

5.   Shi WT, Forsberg F, Bautista R, Vecchio C, Bernardi R, Goldberg BB.  Image enhancement by acoustic conditioning of ultrasound contrast agents. *Ultrasound Med Biol*, 30:191 – 198, 2004.

6.   Chatterjee D, Sarkar K.  A Newtonian rheological model for the interface of microbubble contrast agents. *Ultrasound Med Biol,* 29:1749-1757, 2003.

7.   Sarkar K, Shi WT, Chatterjee D, Forsberg F.  Characterization of ultrasound contrast microbubbles using in vitro experiments and viscous and viscoelastic interface models for encapsulation. *J Acoust Soc Am,* 118: 539-550, 2005.

8.   Sarkar K, Jain P.  Growth and dissolution of a shelled bubble applicable in the medical field.  Submitted to *J Acoust Soc Am*, May, 2006.

9.   Chatterjee D, Jain P, Sarkar K.  Ultrasound–mediated destruction of contrast microbubbles used for medical imaging and drug delivery. *Phys. Fluids*, 17:100603 – 100603-8, 2005.

10.  Forsberg F, Shi WT, Knauer MM, Hall AL, Vecchio C, Bernardi R.  Real time excitation enhanced ultrasound contrast imaging. *Ultrasonic Imaging*, 27: 65-74, 2005.

11.  Kabalnov A, Klein D, Pelura T, Schutt E, Weers J.  Dissolution of multicomponent microbubbles in the blood stream: 1. Theory. *Ultrasound Med. Biol*., 24: 739-749, 1998.

12.  Forsberg F, Basude R, Liu JB, Alessandro J, Shi WT, Rawool NM, Goldberg BB, Wheatley MA.  Effect of filling gasses on the backscatter from contrast microbubbles: theory and *in vivo* measurements. *Ultrasound Med. Biol.*, 25: 1203 - 1211, 1999.

# Appendix I

The Statement of Work from the original proposal:

*Task 1:* To investigate activation-induced scattering enhancement at different center frequencies, amplitudes, and shapes (or lengths) of activation pulse sequences (Months 1-18):

    a. Construct an *in vitro* experimental system for ultrasonically activating contrast microbubbles and measuring the resulting changes in backscattering (Months 1-2).

    b. Design and develop numerical codes for a theoretical model describing the dynamics and instability of ultrasonically activated contrast microbubbles (Months 1-6).

    c. Calculate the behavior of individual contrast microbubble and the collective behavior of contrast microbubble populations (Months 6-18).

    d. Measure changes in backscattered fundamental, second and sub-harmonic signals before and after activation (Months 3-18).

    e. Predict optimal contrast agents for ultrasound-activated contrast imaging accordingto the numerical simulations (Months 12-18)

    f. Select optimal contrast agents for ultrasound-activated contrast imaging. The selection is mainly based on experimental measurements (Months 12-18).

    g. Develop activation and imaging strategies, based on both numerical simulations and experimental measurements for the scattering enhancement (Months 12-18).

*Task 2:* To implement ultrasound-activated contrast imaging (Months 18-24):

    a. Produce and evaluate activation-enhanced A-lines in an *in vitro* perfusion phantom using the simple pulse-echo system (Months 18-20).

    b. Optimize activation and imaging strategies, based on *in vitro* phantom measurements and simulations with actual parameters of designated transducers (Months 18-24).

    c. Modify a state-of-the-art ultrasound imaging system to incorporate the ultrasound-activated contrast imaging modality (Months 21-24).

    d. Evaluate the new imaging modality in an *in vitro* perfusion phantom using the modified ultrasound scanner (Months 21-24).

*Task 3:* To validate the clinical potential of ultrasound-activated contrast imaging using an established canine prostate cancer model (Months 25-32):

    a. Create and grow prostate tumors by implanting a Canine Transmissible Venereal Sarcoma (CTVS) cell line into the prostate (Months 25-29).

    b. Produce and evaluate activation-enhanced contrast images of canine prostates with CTVS tumors (Months 26-30).

    c. Perform pathological evaluations of prostate specimens and quantify the microvessel density with immunohistochemical staining (Months 28-31).

    d. Process data and images and write final report (Months 31-32)